AIP | Conference Proceedings

Dynamic heterogeneity in the glass-like monoclinic phases of some halogen methane compounds

M. J. Zuriaga, S. C. Perez, L. C. Pardo, and J. Ll. Tamarit

Additional information on AIP Conf. Proc.

Journal Homepage: http://proceedings.aip.org/

Journal Information: http://proceedings.aip.org/about/about_the_proceedings

Top downloads: http://proceedings.aip.org/dbt/most_downloaded.jsp?KEY=APCPCS

Information for Authors: http://proceedings.aip.org/authors/information_for_authors

Dynamic heterogeneity in the glass-like monoclinic phases of some halogen methane compounds

M. J. Zuriaga[1], S. C. Perez[1], L. C. Pardo[2] and J. Ll. Tamarit[2]

[1]*Facultad de Matemática, Astronomía y Física, Universidad Nacional de Córdoba and IFEG-CONICET, Ciudad Universitaria, X5016LAE Córdoba, Argentina.*
[2] *Grup de Caracterització de Materials, Departament de Física i Enginyeria Nuclear, ETSEIB, Diagonal 647, Universitat Politècnica de Catalunya, 08028 Barcelona, Catalonia (Spain)*

Abstract. In this work we study the heterogeneity of the dynamics on the low-temperature monoclinic phases of the simple molecular glassy systems CBr_nCl_{4-n}, $n = 0, 1, 2$. In these systems the disorder comes exclusively from reorientational jumps mainly around the C3 molecular axes. The different time scales are determined by means of the analysis of the spin-lattice relaxation time obtained through Nuclear Quadrupole Resonance (NQR) technique. Results are compared with those obtained from dielectric spectroscopy, from which two $\alpha-$ and $\beta-$relaxation times appear. NQR results enable us to ascribe with no doubt that the existence of two relaxations is due to dynamical heterogeneities which are the consequence of the different molecular surroundings of the molecules in the asymmetric unit cell of systems here studied.

INTRODUCTION

The nature of the dynamics of the liquids and the formation of a glass reveal a rich variety of poorly understood phenomena in chemically very diverse systems. In spite of the diversity, the universality of many observed common features makes the study of the glass formers in general, and the glass state in particular, one of the key unsolved questions in condensed matter physics.[1,2] Although the dynamics slowing down of these systems can be characterized by a quite large number of experimental techniques, those concerning spectroscopic methods are the most utilized. In particular, dielectric spectroscopy is one of the most active in the field characterizing the slowing down dynamics when approaching the glass transition.[3] By such a technique the generalized susceptibility spectra can be determined. Spectra generally consist, at least, on a main or primary or α-relaxation and a secondary or β- or Johari-Goldstein relaxation.[4,5] The α-relaxation is ascribed to the liquid flow process inescapably linked to the translational diffusion in liquid phases or to the orientational diffusion for long-range translationally ordered phases with orientational molecular disorder. As far as the β-relaxation is concerned, although inherent to the glassy state, its origin is still controversial and is one of the most discussed topics within the glassy dynamics field.[6] Disregarding secondary processes due arrangements of internal molecular degrees of freedom given rise to dipole fluctuations, it is usually considered to be related to local motions which seem to remain thermally activated even below the glass-transition. Within the susceptibility scenario β-relaxation can appear as a well-defined peak far away from α- relaxation or as a shoulder into the high-frequency side (excess wing) of the α-relaxation.

One intrinsically linked universal feature to the aforementioned concerns the existence of dynamical heterogeneities, i.e. a heterogeneous distribution of local relaxation times,[7-9] which has been proven experimentally[10,11] and by means of molecular dynamics simulation[12-15] in a large number of quite diverse systems. The existence of spatial heterogeneous dynamics appears when intrinsically exponential processes with different characteristic time scales superpose. Nevertheless, from an experimental point of view, virtually the same results can emerge when nonexponential relaxations due to the superposition of intrinsically different nonexponential processes merge. Both cases can be well differentiated only when the superposed nonexponential processes are far away from a time scale point of view. Within the "authentic" case of heterogeneity a subset of molecular entities translate (or rotate) much faster than other part of the system.

From an experimental point of view the number of works describing detailed physical information about the dynamical heterogeneities is scarce. On the contrary, computer simulations offer us rich and large physical information concerning the origin of the phenomenon. Even in simple hard-sphere systems

strong anisotropic dynamics has been shown.[15-22] The main idea to bring up dynamical heterogeneity is to "select" the subset of relaxing entities in a system that moves (translational or rotational diffusion) faster or slower than the average of the system and, from a computational point of view to define the pertinent correlations between the displacements of the entities. Here some remarks about the different assumptions concerning dynamical heterogeneity are needed. According to Richter,[7] heterogeneous dynamics is characterized by individual relaxing units having site specific relaxation times. For Cicerone and Ediger[8] the relaxation dynamics for different set of environments is nearly exponential but the relaxation time varies significantly among environments, so a very close notion to that used by Richter, if individuals are equivalent to environments. According to Berthier,[9] dynamics heterogeneity refers to the existence of transient spatial fluctuations in the local dynamical behavior, in such a way that different regions might relax in a different manner and at a different rate giving rise to a very broad distributions of relaxation times and strongly non-exponential. Whatever the different description has been proposed for different authors, the least common multiple for dynamical heterogeneity is the existence of individuals (or set of environments or regions) in which the relaxation time (exponential or non-exponential) is different.

From an experimental point of view, many experimental techniques can account the dynamics of the average of the system, but only local techniques can mark off the entities with their own characteristic time. In order to gain some insight on the microscopic origin of the dynamic heterogeneities a pertinent system choice is a *sine qua non* condition. It is with this goal in mind that a reduction of the complexity of the system would provide irrefutable proofs of the existence of dynamical heterogeneity. Thus, canonical glasses are obtained from supercooled liquids in which both translational and orientational degrees of freedom are frozen. In a more restrictive scenario, orientational glasses can be obtained by cooling (or pressurizing) the ergodic orientational disordered phase present in plastic phases (orientationally disordered) with a well-defined regular lattice formed by the center of mass of the molecules. For these cases, only rotational diffusion exists, resulting in a diminution of the degree of complexity when compared with canonical glasses. A strong reduction of the complexity can be achieved by diminishing the number of orientational sites in which the orientation of the entities can appear. Such a case appears in the low-temperature phase of some halogen methane derivatives and in the low-temperature phase of adamantanone,[23] among other. For the former case, the tetrahedral molecules of the series CBr_nCl_{4-n}, $n = 0, 1, 2$) it is known the existence

of a monoclinic lattice (C2/c) with Z=32, but with the asymmetric unit formed by 4 molecules. This fact means that 4 different molecules are nonequivalent from the point of view of the environment and, thus, from the interaction characteristics.[24,25]

Due to the isostructural lattice for all the aforementioned molecules, it is compulsory that for n=1 and n=2 compounds the halogen (Cl and Br) atoms to be disordered with respect to the occupancy of their sites. For these "ordered" phases of $CBrCl_3$ and CBr_2Cl_2 compounds the molecules are disordered so that halogen sites have fractional occupancies of 0.75 and 0.25, for $CBrCl_3$, and 0.50, forCBr_2Cl_2, for each of Cl and Br atoms, respectively. Thus, it was early shown that both compounds undergo a glass transition at about 90 K associated with the freezing of exchange positions between Cl and Br atoms.[26] The different dynamical exhibited by the molecules of the asymmetric unit gives rise to the appearance of the universal α-and β-relaxations. These relaxations come from the reorientation of the dipole due to the occupational site disorder. **Figure 1** depicts the CCl_4 molecule with the C_{3v} axes around which rotational jumps with different w_i (i=1,…, 4) probability can appear. Possible rotations around the C_{2v} axes can be discarded as it has been recently demonstrated (in the liquid state) by a calculation of the energy barriers concerning such rotations.[27]
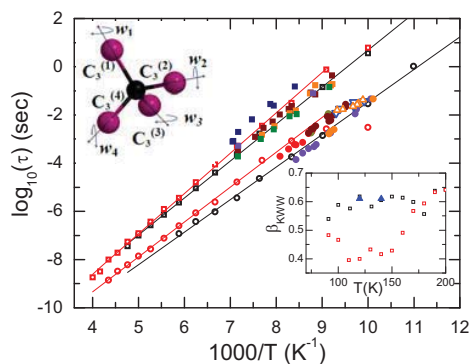

FIGURE 1. Reorientational relaxation times τ_α (empty squares) and τ_β (circles) for CCl_2Br_2 (red) and CCl_3Br (black) obtained from dielectric spectroscopy from ref. 23 and NQR τ_c correlation times (filled squares and circles) for CCl_4 from ref. 28. Empty blue and orange triangles NQR correlation times for CCl_3Br and CCl_2Br_2.Bottom-right inset shows the β^{KWW} stretched exponent of the stretched relaxation function for $CBrCl_3$ (empty black squares) and CBr_2Cl_2 (empty red squares). Top-left inset sketches the CCl_4 molecule indicating the C_{3v} symmetry axes.

When the Cl atoms of the CCl$_4$ molecule are substituted by Br atoms (CBrCl$_3$ and CBr$_2$Cl$_2$ molecules), a dipole moment is provided, making feasible the study of the reorientational dynamics by dielectric spectroscopy (see τ_α and τ_β relaxation times in **Figure 1**). Such study showed the existence of a slower (α-) and a faster (β-) relaxations with noticeable different strength (β- relaxation strength is around two orders of magnitude smaller than that of the α-relaxation). The conclusions of the preceding work established that, in fact, the existence of non-equivalent molecules with respect to their molecular environments give rise to reorientational jumps at different time scales from which both relaxations originate. Nevertheless, dielectric spectroscopy can only account for the existence of two different dynamics of the jumps, without details about the physics behind. In a recent work, a fine analysis of nuclear quadrupole resonance (NQR) measurements enable to assign the origin of both relaxations to the dynamics of three (for the α-relaxation) and one (for the β-relaxation) molecules in the asymmetric unit. Moreover, the Kohlrausch–Williams–Watts stretched exponent β^{KWW} describing the extension of the distribution of the different time scales, through the stretched relaxation function, $\varphi(t) \propto \exp(-t/\tau)^{\beta^{KWW}}$, for the α-relaxation of both CBrCl$_3$ and CBr$_2$Cl$_2$ materials, was found below 0.6 (see inset in **Figure 1**), thus providing evidences of strong local heterogeneities. Although the main disadvantage of the NQR concerns the reduced time scale window, far away from the broad range provided by dielectric spectroscopy, it enables to follows the spin-relaxation time of each nonequivalent ^{35}Cl nucleus and then to bring out the details of the different physical time scales.

In the present work we provide additional details based on the NQR measurements in order to quantify the dynamical heterogeneity of the rotational dynamics in the low-temperature monoclinic phases close to the glass transition temperature of these compounds. For CCl$_2$Br$_2$ and CCl$_3$Br we show additional NQR measurements, while for CCl$_4$ the set of measurements described in ref. 28 were used.

EXPERIMENTAL

Nuclear quadrupole resonance (NQR) is a technique based on the interaction between the nuclear electric quadupolar moment and the electric field gradient (EFG) at the nuclear site.[29] This technique is quite similar to the NMR technique, for which the energy levels are generated by the interaction of the nuclear magnetic moment with an external magnetic field. When some kind of disorder is present, the resonance line which reflects the local structural order is considerably broadened.[30] Since the magnitude of the EFG at the nuclear site is an extremely sensitive function of its near-neighbor environment, NQR is an appropriate technique to characterize different solid phases.

The ^{35}Cl NQR transition frequencies and spin lattice relaxation times T_1 were measured using a homemade Fourier transform pulse spectrometer. The samples were sealed under vacuum and their temperature was controlled within 0.1 K using a homemade cryostat. The NQR spectra in crystalline CCl$_4$ were obtained from the Fourier transform of the free induction decay. The broad spectra of CCl$_3$Br and CCl$_2$Br$_2$ were obtained using the reconstruction nuclear spin-echo Fourier transform mapping spectroscopy method (NSEFTMS).[31]

The spin lattice relaxation times were obtained from the exponential evolution of the NQR signal, measured by using the inversion-recovery ($\pi - t - \pi/2$) sequence. In CBrCl$_3$ and CBr$_2$Cl$_2$, T_1 was measured at the central frequency of the NQR spectrum, while in CCl$_4$, T_1 was measured for each line in the spectrum in order to obtain microscopic dynamic information.

CCl$_3$Br (99%), and CCl$_4$ (99%) compounds were obtained from Across and used as purchased, while CCl$_2$Br$_2$ (98%) was obtained from Aldrich Chemical Co. and fractionally distilled

RESULTS AND DISCUSSION

Because the number of lines in ^{35}Cl NQR spectrum is proportional to the number of non-equivalent chlorine nuclei in the asymmetric unit of the crystal cell and thearea under the NQR line is proportional to the number of resonantnuclei at that frequency, the CCl$_4$ spectra must show 16 lines, being that the asymmetric unit contains 4 molecules, each one with four Cl atoms. **Figure 2** depicts speaking examples at different temperatures for CCl$_4$ in the low-temperature monoclinic C2/c phase.

As far as the CCl$_2$Br$_2$ and CCl$_3$Br are concerned, the occupancy site disorder due to the ubiquitous compatibility between the molecular symmetry (C$_{2v}$ and C$_{3v}$, respectively) and the site symmetry corresponding to the C2/c unit cells for both compounds (isostructural to that of CCl$_4$) [24,25] gives rise to broad ^{35}Cl NQR spectra. Some examples are given in **Figure 2**.

^{35}Cl NQR frequencies were measured and the result is depicted in **Figure 3** (see the numbered 16 lines in **Figure 2**). The ^{35}Cl NQRfrequencies which decrease monotonically with temperature due to an average effect of the molecular torsional oscillations in

the EFG, were fitted by means of the Bayer–Kushida model:[29]

$$v_Q\left(T\right) = v_o\left(1 - \frac{3}{2}\frac{\hbar}{I\omega_t}\coth\left(\frac{\hbar\omega_t}{2k_BT}\right)\right) \quad (1)$$

where v_0 is the limiting static value of the resonance frequency corresponding to the NQR frequency of a hypothetical rigid lattice, I is an effective moment of inertia[32] and $\omega_t = \omega_0(1-gT)$ is an average torsional frequency assuming that the anharmonic effects are contained into the linear temperature-dependence of ω_t.[33]
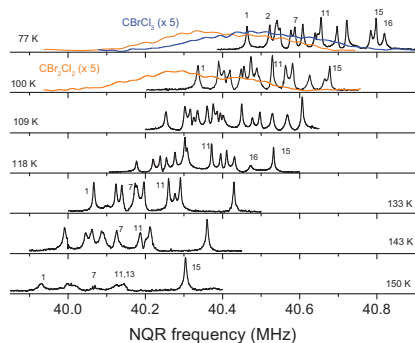
Temperature-dependence of spin-lattice relaxation times for molecular crystals and rigid molecules, as those here concerned, can be split in two terms describing the molecular librations, $\left(T_1\right)_{libr}$, and the reorientational mechanism, $\left(T_1\right)_{reor}$. Thus,

$$T_1^{-1} = \left(T_1^{-1}\right)_{libr} + \left(T_1^{-1}\right)_{reor} \quad (2)$$

The temperature dependence of the molecular librations are commonly expressed by $\left(T_1^{-1}\right)_{libr} = aT^{\gamma}$.

FIGURE 2. Representative ^{35}Cl NQR spectra at different temperatures for CCl$_4$ (black) and for CCl$_2$Br$_2$ (orange) and CCl$_3$Br (blue), the last scaled by a factor 5.
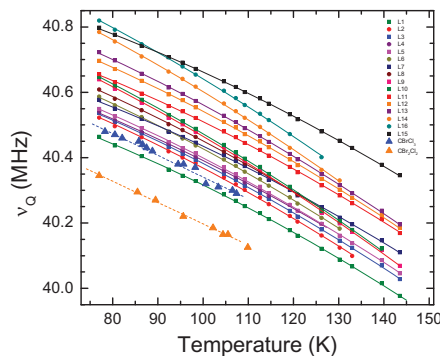

FIGURE 3. Results for the ^{35}Cl NQR quadrupole frequencies as a function of temperature obtained from the set of resonant lines of the spectra in **Figure 2** for CCl$_4$ (circles). Triangles indicate the central ^{35}Cl NQR frequencies for CBrCl$_3$(blue triangles) and for CBr$_2$Cl$_2$(orange triangles).

It can be noticed that some lines cross and some other vanish or widen when temperature increases. This experimental fact reveals the speed up of the molecular reorientation. One of the most important evidence emerging from the temperature-dependence of the quadrupole frequencies is that, despite the monotonous decrease with increasing temperature for all of them, the rate is different and, more into specifics, they can be grouped into some subsets, which clearly indicates the existence of different dynamical behaviors within the system. The fits provide the average libration frequency $\omega_0(\approx 47\mathrm{cm}^{-1})$ and parameter g ($\approx 1.1\text{-}1.6\ 10^{-3}$ K^{-1}) which match perfectly with those previously reported from IR and Raman spectroscopy ($\bar{\omega}_{libr} \approx 50cm^{-1}$ and $g \approx 1_\times 10^{-3}$K^{-1}).[34,35]

The dynamics of the system has been accounted by means the spin-lattice relaxation time (T_1). By the inversion recovery sequence described in Section 2, the nuclear magnetization follows the exponential relation $M = M_o\left(1 - 2e^{-t/T_1}\right)$. The results for the spin-lattice relaxation time T_1 were obtained as a function of temperature from 77 to 145 K only for 8 lines over the 16 due to the overlap of lines.
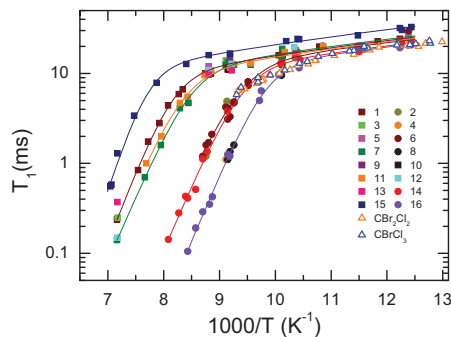

FIGURE 4. Spin-lattice relaxation time as a function of temperature for CCl$_4$ (full symbols) and for CCl$_2$Br$_2$ (orange triangles) and CCl$_3$Br (blue traingles). Lines are fits through eq. (2).

The value of γ is found to be around 2,[36] which means that the relaxation time at not very low temperatures is governed by molecular vibrational mechanisms. This scaling is clearly evidenced in the low-temperature

region of **Figure 4**. On the grounds of the standard model described in ref. 37, the second term in eq. (2) describing the reorientational mechanism can be written as

$$\left(T_1^{-1}\right)_{reor} = b\,\tau_c^{-1} = b\,\tau_o^{-1} \exp\left(-\frac{E_a}{k_B T}\right) \qquad (3)$$

where τ_c is the correlation time, E_a is the activation energy of the reorientation and b is a constant. The high-temperature region in **Figure 4** reveals the Arrhenius behavior of the spin-lattice relaxation time. By inserting eq. (3) in eq. (2) and replacing the $\left(T_1\right)_{libr}$ by its temperature dependence, relaxation times were fitted for CCl_4. Activation energy was found $E_a = 28.5 \pm 1.5\ kJ\ mol^{-1}$ for the almost all of analyzed lines (except for line 15, 15% larger), whereas the reciprocal of the prefactor $\tau_o b^{-1}$ is ranged between $2 \cdot 10^{-15}$ s and $3 \cdot 10^{-17}$ s. These values for the slowest and fastest dynamical scales highlight once again the dynamical heterogeneity of the system.

As for the reorientational times of $CBrCl_3$ and CBr_2Cl_2, due to the narrow available temperature range (between 77 and 107 K), values were obtained by successive fits, first subtracting the librational contribution and thereupon by fitting the reorientational mechanism. The results are reported in **Figure 5** for all the analyzed correlation times. This figure provides the most clear experimental evidence of the heterogeneous dynamics because the NQR technique can feel the different time scales (heterogeneity) arising from the different molecular environment of the molecules in the asymmetric unit. Four different dynamical groups of relaxation times appear for CCl_4 (with virtually the same temperature dependence), the signature of the heterogeneity. As for $CBrCl_3$ and CBr_2Cl_2, it can be seen that the relaxation times spread along different well-defined relaxation times for CCl_4, as a consequence of the additional statistical disorder which can increase the spatial heterogeneity.

In fact, relaxation times for the α-and β-relaxations obtained from dielectric spectroscopy (**Figure 1**) and those obtained from NQR describe the same dynamics, but the former technique can only account for the dipole fluctuations due to the dynamic exchange between Cl and Br atoms, and thus, the two relaxations are somehow an average. The existence of dynamical heterogeneity can be suspected in the imaginary part of the susceptibility through the shape of the dielectric spectra. From our previous work[28], in which the dielectric spectra were fitted by means of the Havriliak-Negami (HN) function, the β_{KWW} (Kohlrausch–Williams–Watts) stretched exponent of the stretched relaxation function, $\varphi(t) \propto \exp(-t/\tau)^{\beta KWW}$,

was determined. Values of the exponent were around 0.6 for $CBrCl_3$ and 0.5 for CBr_2Cl_2 (see inset in **Figure 1**). Such small values are an irrefutable proof of the existence of strong local heterogeneities due to different dynamics. NQR technique provides, in addition, the magnitude of such heterogeneities, which, surprisingly enough are the same for the three involved compounds.
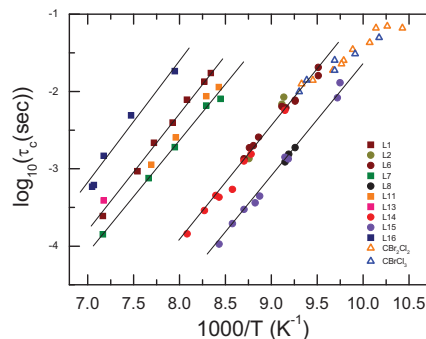

FIGURE 5. Correlations times for the reorientational mechanism obtained from fits of T_1 according to eq. (3) for CCl_4 and for $CBrCl_3$ (empty orange triangles) and CBr_2Cl_2 (empty blue triangles).

By knowing the complete scenario of the relaxation times (we had only access to 8 over 16 resonant lines), the correlation decay, $\varphi(t)$, could be reconstructed by the superposition of exponentials with the appropriate probability density $g(\tau)$:
$$\varphi(t) = \int_0^\infty g(\tau) \cdot e^{-t/\tau} d\tau = <e^{-t/\tau}>.$$ In the present case, we were not able to do such a reconstruction, because the probability functions $g(\tau)$ are in need for the whole relaxation times (corresponding to the 16 chlorine atoms of the asymmetric unit). Nevertheless, being aware of the limited information, we have determined the correlation function with seven of the longest NQR relaxation times in order to estimate the β_{KWW} parameter for the slowest α-process. The obtained values between 120 and 140 K are around 0.6, which is certainly close to the values determined from dielectric spectroscopy as shown in the inset of **Figure 1**.

To deepen the knowledge of the particular reorientational mechanisms of the involved molecules, we will consider here the different molecular rotations and evaluate the balance of probabilities around the different molecular axes. In previous works both molecular dynamics simulations[38] and reverse MonteCarlo methods have described the influence of

63

steric and electrostatic interactions on these materials.[27] As for the later, the analysis of the short-range order in the liquid state concluded that neither the interaction between dipoles (for the $CBrCl_3$ and CBr_2Cl_2 cases) not the steric differences have noticeable influence to modify the local structure appearing for CCl_4 molecules. In addition, one of the most important conclusions of that work states that the energy barriers for rotations about the C_{2v} axes are much higher than those about the C_{3v} axes. Similar results were found in the low-temperature phase of $CBrCl_3$ by molecular dynamics simulations and, even more, for CCl_4 it was clearly shown up that below 160 K such a C_{2v} rotations did not take place.[39] On the grounds of these well-established hypothesis, we have taken advantage from the fact that, in spin-lattice relaxation measurements, nuclear magnetization is proportional to the nuclear spin polarization. Thus, according to the existing models[34] the time dependence of the nuclear spin polarization can be described as:

$$\frac{d\left(P^{\nu} - \left\langle P^{\nu} \right\rangle_{eq}\right)}{dt} = \sum_{\nu'}\left[\frac{1}{3}\left(3\cos^2\theta_{\nu\nu'} - 1\right)\right]\left(w_{\nu\nu'}P^{\nu'} - w_{\nu'\nu}P^{\nu}\right) - \frac{3}{2}\sum_{\nu'}w_{\nu'\nu}\left(1 - \cos^2\theta_{\nu\nu'}\right)\left(P^{\nu} - \left\langle P^{\nu} \right\rangle_{eq}\right) \qquad (4)$$

where P^{ν} is the polarization component, ν represents the site that the nucleus can occupy in the molecule ($\nu = 1,...4$), $w_{\nu\nu'} = w_{\nu'\nu}$ is the transition probability of the nucleus from site ν to site ν' and $\theta_{\nu\nu'}$ is the angle (tetrahedral angle, 109.47°) between C-Cl bonds in sites ν and ν'. Discarding the C_{2v} rotations as previously explained, only four different probabilities around the C_3 axes will be defined and denoted w_i (i =1-4) (see top inset in **Figure 1**), which assuming perfect tetrahedral symmetry of CCl_4 the must be correlated as $w_{12} = w_3 + w_4$, $w_{13} = w_2 + w_4$ and $w_{14} = w_2 + w_3$. Obviously, if Cl nuclei can jump from one site to another by more than one mechanism (rotational jumps about the four C_3 axes of the molecule), then $w_{\nu\nu'} = \sum_m w_{\nu\nu'}^{(m)}$, where $w_{\nu\nu'}^{(m)}$ is the transition probability of the molecule by the mechanism "m" between the position ν' and ν of the nucleus. Expression (4) has a matricial form, $\dot{\mathbf{P}} = \mathbf{\Lambda P}$, $\mathbf{P}$ being the four-components polarization vector and $\mathbf{\Lambda}$ is the relaxation matrix (for which the inverse of the eigenvalues are the decay constants τ). The obvious solution for the differential equation is $\mathbf{P}(t) = \mathbf{R}^{-1}\exp(\mathbf{\Lambda}_R t)\mathbf{R}\mathbf{P}(0)$ (where $\mathbf{R}$ is the matrix which diagonalizes $\mathbf{\Lambda}$), and the initial conditions for the univocal solution are 0 and 1 depending on whether the nuclear spin site ν is polarized. The time dependence of $\mathbf{P}(t)$ can be calculated for different w_i/w_j

ratios within a usual experimental time range between 0 and t', with the constraint that $P(t') = 0.02 \cdot P(0)$, for different initial conditions.

Some examples of the calculations of the decay constant τ are displayed in **Figure 6** for three different relations w_2/w_1 ($w_2 << w_1$, $w_2 = w_1$ and $w_2 << w_1$) as a function of the w_3/w_1 and w_4/w_1 ratios. Two conclusions can be derived for such examples: (i) when all w_i are equals (see panel b), there is only one decay constant τ, and (ii) when only one $w_k >> w_i$ (i = 1…4, i≠ k) there is one long τ and three short τ's, which may differ by many orders of magnitude and the ratio τ_{long}/τ_{short} is proportional to w_i/w_k. In this case, the shortest times differ by a factor between 2 and 3. Whatever the case different from the previous limiting cases, there are four distinct decay times that differ by a factor no greater than 2.5.
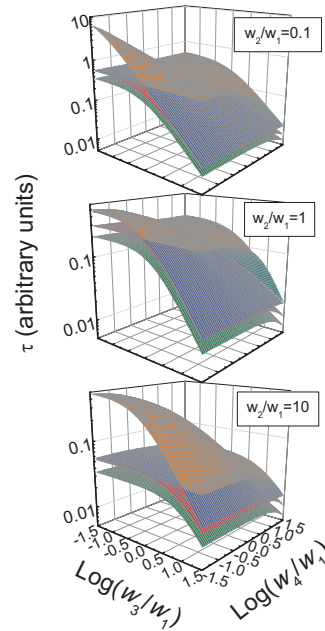

FIGURE 6. Decay constants τ (inverse of eigenvalues of $\mathbf{\Lambda}$) for the ratios w_2/w_1: a) $w_2/w_1=0.1$, b) $w_2/w_1=1$, c) $w_2/w_1=10$ as a function of the w_3/w_1 and w_4/w_1 ratios.

Then the τ_c obtained from NQR data for each molecule will be: one (if all w_i are equal), four similar τ_c (if all the w_i are quite different) or one long τ_c and three shorts τ_c's (if there is preferred rotation about an axis).

In the hypothetical case that all the molecules would have the same dynamics, one of the situations mentioned above should be observed. The results in

Figure 5, makes clear that this is not the case and therefore there are two or three groups of molecules with different dynamics.

Molecular dynamics simulations in the low-temperature monoclinic phase of CCl_4 have shown that the four molecules of the asymmetric unit cell show reorientational dynamics with different correlation times and, in particular, that only one molecule reorients preferably around one of the reorientational C_{3v} axes.

CONCLUDING REMARKS

In this work we have shown that on the low-temperature monoclinic phases of the simple molecular glassy systems CBr_nCl_{4-n}, $n = 0, 1, 2$, the disorder is exclusively coming from reorientational jumps on two main time scales due to the different molecular surroundings of the molecules. Nevertheless, the features of the dynamics of these "well-ordered" glassy systems are perfectly in agreement with those of more typical canonical glasses. More into specifics, we demonstrate that the α- and β-relaxation processes appearing in the dielectric spectra correspond to the different time scales (heterogeneity) due to the different molecular environments of the four nonequivalent molecules in the asymmetric unit of the lattice. Although the time window accessible by NQR is less wide than that of dielectric spectroscopy, more detailed information can be reached and, in particular, the reorientational jumps of the molecules around different C_{3v} axes can be accurately investigated.

Although the features of the dynamics of these "well-ordered" glassy systems are in agreement with those of canonical glasses, the question is whether they also show the canonical low-temperature thermal properties that are found for all amorphous and OD glassy systems.[40] The conventional wisdom at present is that the same distribution of local atomic environments that provides thermally-activated hopping (rotational or translational or both) and thus the secondary (β-) relaxation near the glass transition, also provides glassy tunneling two-level systems at very low temperature manifested by the linear term in specific heat and the T^2 term in thermal conductivity, both considered as fingerprints for all amorphous systems and some disordered crystals. At present we are currently investigating such low-temperature properties on these "well-ordered" glasses. At the same time, it would be interesting to find additional molecular systems in which "ordered" phases exhibit some kind of disorder, in such a way that glass properties can emerge. These systems would provide the opportunity to find out new experimental (and simulations) ways to describe accurately the physical properties of the system and, thus, to figure out some of the claimed secrets of the glass state. Within the same purpose, a recent work on the low-temperature phase of adamantanone has been recently published.[23] In this case the dielectric spectra for the "ordered" phase exhibit the universal coexistence of α- and β-relaxation processes, identified as a strongly restricted reorientational motion (α-relaxation) and an original Johari-Goldstein β-relaxation.

All in all, by diversifying the kind of systems under study we can learn much more than intensifying the number of experimental systems under scrutiny.

ACKNOWLEDGMENTS

REFERENCES

1. P. W. Anderson, Science, **267**, 1615-1616 (1995).
2. P. G. Debenedetti and F. H. Stillinger, Nature **410**, 259-267 (2001).
3. F. Kremer and A. Schoenhals, *Broadband Dielectric Spectroscopy*, Berlin: Springer-Verlag, 2003.
4. R. Brand, P. Lunkenheimer and A. Loidl, J. Chem. Phys. **116**, 10386-10401 (2002).
5. G. P. Johari and M. Goldstein, J. Chem. Phys. **53**, 2372-2388 (1970).
6. K. L. Ngai, Phys. Rev. E 57, 7346-7349 (1998).
7. R. Richter, J. Phys.: Condens. Matter **14**, R703-R738 (2002).
8. M. T. Cicerone and M. D. Ediger, J. Chem. Phys. **103**, 5684-5692 (1995).
9. L. Berthier, Physics **4**, 42 (2011).
10. M. D. Ediger, Annu. Rev. Phys. Chem. **51**, 99-128, (2000).
11. H. Sillescu, J. Non-Cryst. Solids **243**, 81-108 (1999).
12. R.Palomar and G. Sesse, J. Phys. Chem. B **109**, 499-507 (2005).
13. R.Palomar and G. Sesse, Phys. Rev. E 75, 011505 (2007).
14. K. L. Ngai and S. Capaccioli, J. Phys. Chem. B **108**(30), 11118–11123 (2004).
15. C. M. Roland, D. Fragiadakis, D. Coslovich, S. Capaccioli and K. L. Ngai, J. Chem. Phys. **133**(12), 124507 (2010) .
16. B. Doliwa and A. Heuer, Phys. Rev. Lett. **80**, 4915-4918 (1998).
17. W. Kob, C. Donati, S. J. Plimpton, P. H. Poole, and S. C. Glotzer, Phys. Rev. Lett. **79**, 2827-2830 (1997) .

18. C. Donati, S. C. Glotzer, P. H. Poole, W. Kob and S. J. Plimpton, Phys. Rev. E **60**, 3107-3119 (1999).
19. M. Scott Shell, P. G. Debenedetti, and F. H. Stillinger, J. Phys.: Condens. Matter **17**, S4035 (2005).
20. J. Qian, R. Hentschke, and A. Heuer, J. Chem. Phys. **110**, 4514-4512 (1999).
21. M. G. Mazza, N. Giovambattista, F. W. Starr, and H. E. Stanley, Phys. Rev. Lett. **96**, 057803 (2006).
22. R. Palomar and G. Sesé, J. Phys. Chem. B **109**, 499-507 (2005).
23. M. Romanini, Ph. Negrier, J. Ll. Tamarit, S. Capaccioli, M. Barrio, L. C. Pardo, and D. Mondieig, Phys. Rev. B **85**, 134201 (2012).
24. M. Barrio, J.Ll. Tamarit, Ph. Negrier, L.C. Pardo, N. Veglio, D. Mondieig, New J.Chem. **32**, 232-239 (2008).
25. B. Parat, L.C. Pardo, M. Barrio, J.Ll. Tamarit, Ph. Negrier, J. Salud, D.O. López, D.Mondieig, Chem. Mater. **17**, 3359-3365 (2005).
26. T. Ohta, O. Yamamuro, and T. Matsuo, J. Phys. Chem. **99**, 2403-2407 (1995).
27. Sz. Pothoczki, A. Ottochian, M. Rovira-Esteva, L. C. Pardo, J. Ll. Tamarit, G. J. Cuello, Phys. Rev B **85**, 014202 (2012).
28. M. Zuriaga, L. C. Pardo, P. Lunkenheimer, J. Ll. Tamarit, N. Veglio, M. Barrio, F. J. Bermejo, and A. Loidl, Phys. Rev. Lett. **103**(7), 075701 (2009).
29. H. Chihara and N. Nakamura, in Advances in Nuclear Quadrupole Resonance, edited by J. A. S. Smith (Heyden, London, 1980), Vol. 4,p. 1.
30. A. P. Bussandri, M. J. Zuriaga, and C. A. Martin, J. Phys. Chem. Solids **59**, 201-209 (1998).
31. A. P. Bussandri and M. J. Zuriaga, J. Magn. Reson. **131**(2), 224–231(1998).
32. S. Cohen, R. Powers, and R. Rudman, ActaCrystallogr., Sect. B **35**(7),1670–1674 (1979).
33. A. Anderson, B. H. Torrie, and W. S. Tse, Chem. Phys. Lett. **61**(1), 119–123 (1979).
34. R. Brown, J. Chem. Phys. **32**(1), 116-118 (1960)
35. A. Anderson and B. Torrie, J. Mol. Struc. **143**, 95–100 (1986).
36. R. C. Zamar and C. E. González, Phys. Rev. B **51**(2), 932–944 (1995).
37. S. Alexander and A. Tzalmona, Phys. Rev. **138**(3A), A845-A855 (1965).
38. N. B. Caballero, M. Zuriaga, M. Carignano, and P. Serra, J. Chem. Phys. **136**, 094515 (2012).
39. M. Zuriaga, M. Carignano and P. Serra, J. Chem. Phys. **135**(4), 044504 (2011).
40. R.C. Zeller and R.O. Pohl, Phys.Rev. B **4**, 2029-2041 (1979).